EXPERIMENTAL INVESTIGATION OF GEOGRID REINFORCED SOIL UNDER PLANE STRAIN CONDITIONS

F. Jacobs[1], A. Ruiken[2], and M. Ziegler[1]
[1]Geotechnical Engineering, RWTH Aachen University, Germany; Tel: +49-241 8025254;
Fax: +49-241 8022384; Email: jacobs@geotechnik.rwth-aachen.de, ziegler@geotechnik.rwth-aachen.de
[2]Wayss & Freytag Spezialtiefbau GmbH, Germany,
formerly Geotechnical Engineering, RWTH Aachen University; Email: axel.ruiken@wf-ib.de

ABSTRACT

The principle compound behavior of geogrid reinforced soil is being investigated at RWTH Aachen University. For this purpose, a laboratory apparatus has been developed that allows biaxial compression testing of geogrid reinforced soil. To study the compound stress-strain behavior and the complex interaction mechanisms between soil and the geogrids in a non-scaled ratio, the apparatus admits large scale testing of specimens with dimensions of 800 x 820 x 460 mm³ (H x W x D). Furthermore, it has a transparent side wall to determine the reinforcing effect to the kinematic behavior during compression. The tests are being carried out under plane strain conditions with constant confining pressures applied via vacuum. In this paper, the results of first series of biaxial compression tests are presented. Generally, a significant increase in strength has been observed for all reinforced samples due to the confining effect of the geogrids. With an initial test series an appropriate arrangement of the geogrids in the specimens, in terms of the ultimate bearing capacity, the kinematic behavior, as well as the stress distribution at the specimen top surface, has been determined. Subsequent parameters have then been studied with specimens reinforced with two geogrid layers placed at 1/4th and 3/4th of the height. As an important parameter, the tensile stiffness of the geogrids has been varied in a common range between $J_{0\text{-}2\%}$ = 530 and 1650 kN/m. It is shown that an increase of the geogrid tensile stiffness leads to both, a higher stiffness and a higher bearing capacity of the reinforced soil.

Keywords: Geogrid reinforced soil, biaxial compression test, confining effect, plane strain, tensile stiffness

INTRODUCTION

The use of geogrid reinforced soil in geotechnical engineering is already widespread and steadily increasing. So far, design concepts for major applications are mainly based on empirical studies and therefore lead to high safety factors that again lead to ineffective designs. To strengthen the theoretical basis and understanding of the complex compound behavior, a principle investigation of the composite material is necessary.

Generally, for the principle investigation of a soil, element tests are the appropriate tool as the stresses and strains are almost homogenous within the element and can therefore be linked directly. Although an "element" of reinforced soil with several reinforcement layers has a clearly non-homogeneous structure, biaxial and triaxial element tests are still regarded as the most appropriate testing methodology for the investigation of the global stress-strain behavior of geogrid reinforced soil (Ketchart and Wu, 2001).

For the general compound behavior, the effect of particles interlocking with the geogrids is of great importance so that a non-scaled ratio of soil particle size to geogrid aperture size is preferable (Bussert, 2006). In this paper, results of biaxial compression tests with specimen dimensions of 800 x 820 x 460 mm³ (H x W x D) are being presented. These specimen dimensions enable the use of common geogrids with aperture widths of 30 to 40 mm.

The present plane strain condition allows horizontal deformations only in one direction, i.e. the direction of the longitudinal tensile members of the geogrids. The activation of the geogrids, expressed by reinforcement strains and forces, respectively, can therefore be linked directly to an increasing bearing capacity of the reinforced specimen. The prevailing plane strain condition corresponds to the state of strain in major applications of geogrid reinforced soil, e.g. linear structures such as retaining walls and load transfer layers under roads or railway tracks.

LABORATORY TEST SETUP

Testing Apparatus and Procedure

The apparatus in Fig.1 has been developed to carry out large scale biaxial compression tests of geogrid reinforced soil. The results discussed in this paper have been obtained from testing of unreinforced specimens and specimens reinforced with two geogrid layers, as also shown in Fig. 1.

The tests have been carried out under a constant confining stress of $\sigma_3 = 2.5$ kPa that has been applied with a vacuum system. For compression, the specimens have been loaded with a constant strain rate of 1 mm/min ($\dot{\varepsilon}_1 \approx 0.125$ %/min) applied with a stiff loading plate.

A transparent side wall (σ_2-plane) allows for the photographing of the specimens during testing. The kinematic behavior of the specimens has subsequently been evaluated from those photos using the Digital Image Correlation (DIC) method. With a thickness of 106 mm the deflection of the glass wall was reduced to less than 0.1 mm so that the plane strain condition has been preserved throughout testing.

The interfaces between the specimen and the stiff top and bottom plates have been lubricated with a combination of a thin latex membrane and silicone grease (Baysilone®, medium viscous). In accordance with Tatsuoka and Haibara (1985) the resulting contact friction angle has been determined with direct shear tests to less than 2°. For the benefit of a high quality evaluation of the kinematic behavior, the glass side walls have not been lubricated in this study. The contact friction between sand and glass has been determined in advance with direct shear tests to an angle of less than 7°, so that its effect should be considered when transferring the outcomes to in situ conditions.

Materials

The soil used in the tests is a dry uniform-graded medium sand ($d_{50} = 0.5$ mm), classified as "SP" according to the Unified Soil Classification System (ASTM D2487, 2011). It has been deposited with approximately 101 % Proctor density using the rainfall technique described in Ruiken et al. (2010), corresponding to a density of $D = 1.74$ t/m³ and a relative density of $R_D = 89$ %. As reinforcement layers, biaxial polypropylene grids with flat bars and welded junctions have been used. Major properties of these geogrids are listed in Table 1.

Table 1 Geogrid properties

Geogrid	Short term tensile strength *	Tensile stiffness $J_{0\text{-}2\%}$ **	Grid dimension
	[kN/m]	[kN/m]	[mm]
GL-530	≥ 20	530	40
GL-700	≥ 30	700	40
GL-900	≥ 40	900	40
GL-1155	≥ 30	1155	50
GL-1350	≥ 60	1350	40
GL-1650	≥ 80	1650	40

* according to DIN EN ISO 10319 (2008)
** mean values, determined by manufacturers

TEST RESULTS

The reinforcing effect of one and two geogrids, respectively, in comparison with unreinforced specimens was shown in detail in Jacobs et al. (2012) and Ruiken et al. (2012). The total bearing capacity increased by 450 % for a test reinforced with two reinforcement layers compared to an

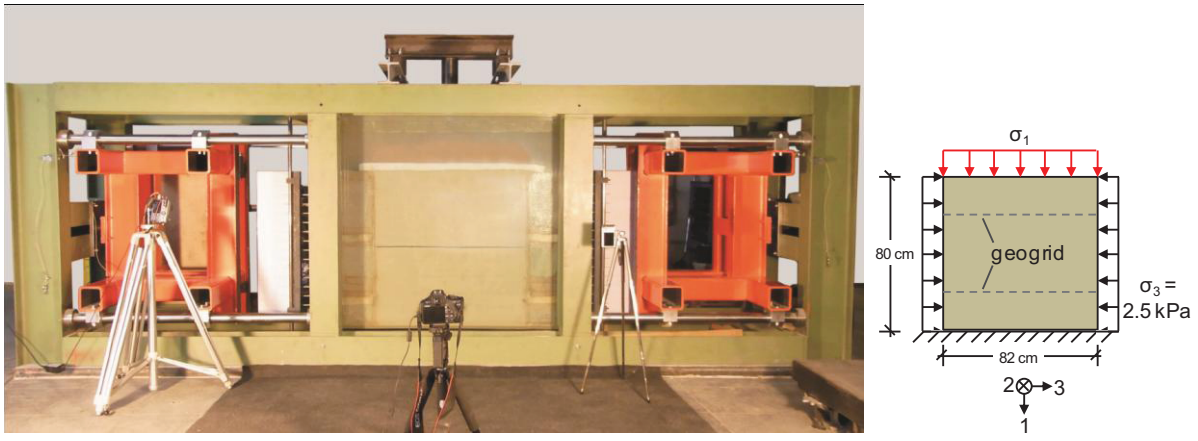

Fig. 1 Laboratory apparatus for large scale biaxial compression testing and sketch of the specimen.

unreinforced specimen. Furthermore, whereas the unreinforced specimen exhibited the highest modulus at the beginning of the test, i.e. E_0, the activation of the geogrids led to an increase of the modulus of the reinforced specimens right after the beginning of the tests.

In conjunction with the activation of the geogrids, a local increase of the lateral pressure, i.e. the minor principal stress σ_3, occurred. This can be concluded from the arching of the soil between the geogrids (to be shown later in Fig. 8), and was also suggested by Vidal (1969) and observed by Peng et al. (2000). The generally increased confining stress has led to much higher bearing capacities and a much more ductile behavior of the reinforced specimens so that the peak strength has been reached at a later compression state ε_1.

Using the DIC method, particle displacements and rotations were quantified. The reinforcement led to a strong reduction of horizontal specimen deformations and to the above mentioned arching of the soil between the reinforcement layers. Instead of only a single connected slip surface across the unreinforced specimen, due to the gradual activation of the geogrids, multiple and variously inclined slip surfaces developed in the reinforced specimens (to be shown later in Figs. 4 and 8).

In this paper, two series of tests reinforced with two geogrid layers (see Tab. 2) have been carried out in order to determine, first, the appropriate geogrid arrangement within the specimens and, second, the influence of the geogrid tensile stiffness on the compound stress-strain behavior.

Table 2 Test program

Parameter	Layer spacing l_v	Geogrid tensile stiffness $J_{0\text{-}2\%}$
	[cm]	[kN/m]
1 Appropriate Geogrid Arrangement	20 - 30 - 40 - 50 - 60	1155
2 Geogrid Tensile Stiffness	40	530 - 700 - 900 - 1350 - 1650

Due to the large specimen height of 800 mm and the low confining stress of 2.5 kPa, the weight of the soil "element" should not be neglected, and is therefore taken into account as an average value determined at mid-height in all analyses as described in Jacobs et al. (2012).

Appropriate Geogrid Arrangement

Ultimate bearing capacity

The results of the above described preliminary tests indicated that the placement of two geogrids within a specimen of the present geometry and boundary conditions may lead to a significant increase of the bearing capacity of the soil. Now, the vertical spacing l_v between the two geogrids has been varied to determine an appropriate arrangement of the two reinforcement layers for the given test setup. Among others, the prevailing boundary conditions comprise lubricated top and bottom plates, an equal height and width of the tested specimens, and that the geogrids have not been fixed at the specimen sides (σ_3-planes). The development of the vertical stress and volumetric strain is presented in Fig. 2 over the vertical strain.

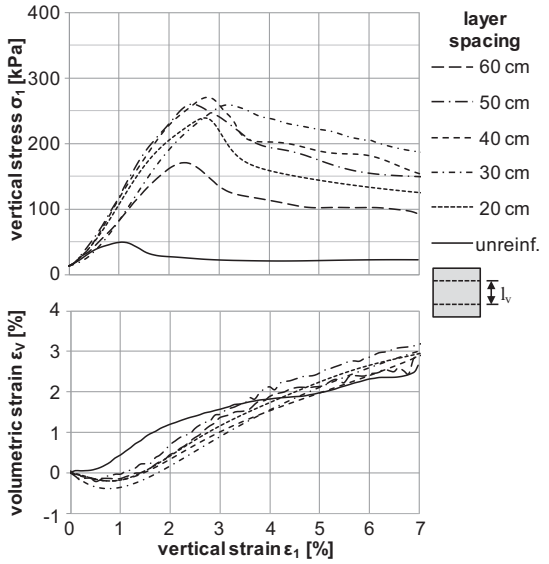

Fig. 2 Stress-strain and volumetric strain behavior of an unreinforced specimen and of specimens reinforced with two geogrid layers (GL-1155) variously vertically arranged.

The ultimate stresses $\sigma_{1,max}$ of the presented tests are summarized in Fig. 3. All tests reach similar ultimate stresses, except for the test with $l_v = 60$ cm. Its low ultimate stress has been confirmed by a second test with $l_v = 60$ cm. In terms of the ultimate bearing capacity, the regular distribution of two geogrid layers with $l_v = 40$ cm, i.e. at 1/4 H and 3/4 H, and the ratio of layer spacing to specimen width $l_v/W = 0.5$ has led to the most effective reinforcement of the specimens under the prevailing boundary conditions.

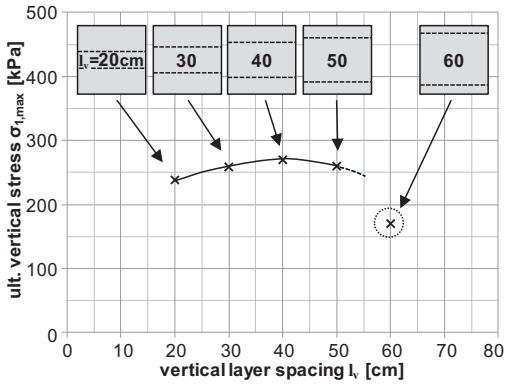

Fig. 3 Ultimate stresses determined with specimens reinforced with two geogrid layers (GL-1155) variously vertically arranged.

Kinematic behavior

The specimen's σ_2-plane has been photographed during the tests to subsequently evaluate the particle displacements and particle rotations with the DIC method. The resulting kinematic behavior of the first test series is illustrated in Fig. 4.

In Fig. 3, it has been shown that the test with a vertical layer spacing of l_v = 60 cm has reached a far lower ultimate vertical stress than all other tests. Now, the kinematics in Fig. 4 show that for this test the lateral soil movement and failure surfaces occurred mainly in the unreinforced soil, avoiding the full activation of the reinforcement layers. Therefore, for the investigated sand-geogrid combination, the results in Fig. 4 indicate that a ratio of $l_v/W = 0.75$ is too high for an effective reinforcement of the specimen under the above described prevailing boundary conditions.

Stress distribution underneath the loading plate

The local vertical stresses between the stiff loading plate and the upper σ_1-surface of the specimens have been measured with a sensitive pressure sensor. In Jacobs et al. (2012), the general validity of the applied method was shown. The measured stresses were in good agreement with the globally applied force and the developing shear zones, evaluated with the DIC method. For comparison, average values over the specimen depth (σ_2-direction) have been determined, leading to the two dimensional plots in Fig.5. For tests with different geogrid arrangements, i.e. various vertical layer spacings, the resulting stress distributions on the top surface of the specimens are compared at three global loading states, i.e. $\bar{\sigma}_{1,axial}$= {40, 125, 210} kPa. Therefore, the resulting stress distributions can actually be compared with each other.

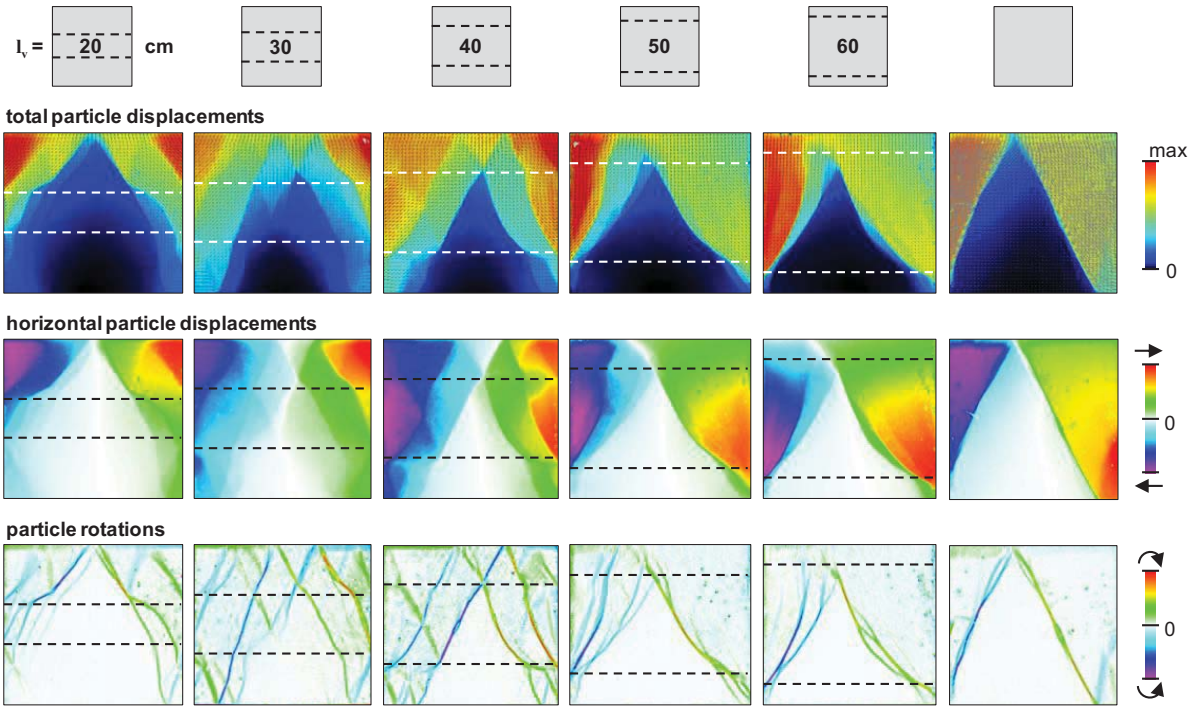

Fig. 4 Kinematic behavior of an unreinforced specimen and those reinforced with two geogrid layers (GL-1155) variously vertically arranged.

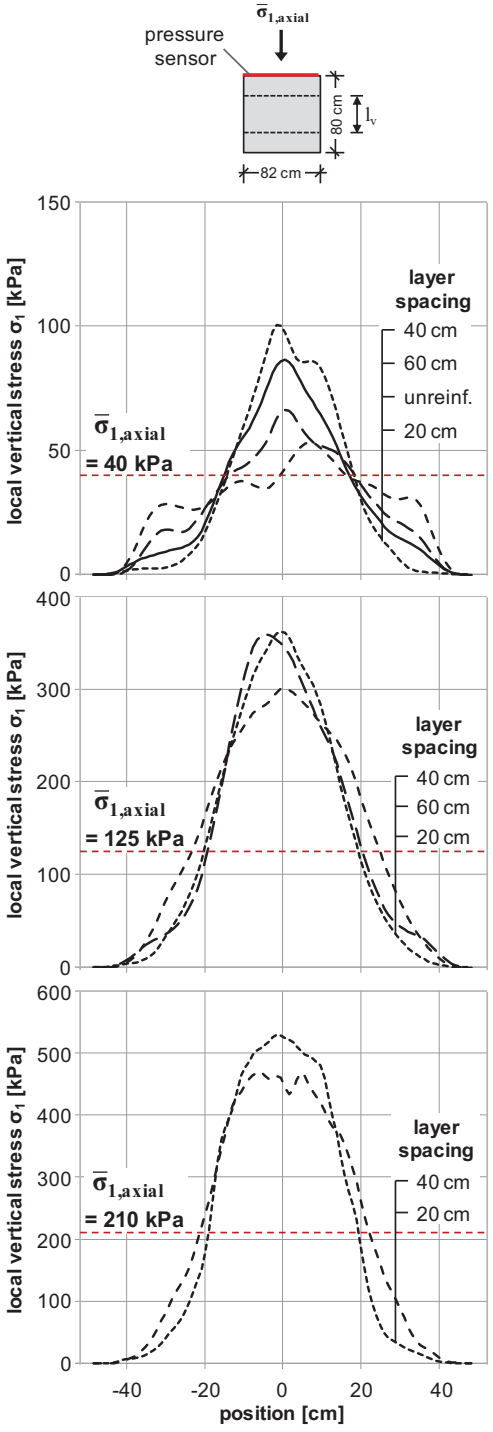

Fig. 5 Local stress distribution on specimen top surface underneath the loading plate for three global loading states (GL-1155).

In the graph of the first loading state ($\bar{\sigma}_{1,axial}$= 40 kPa), it can be seen that for the unreinforced specimen and the one with l_v = 20 cm the load transfer has concentrated in the center of the specimen. The two other tests show a more uniform stress distribution and therefore, the maximum local stresses in the specimens' center are lower.

For the loading state of ($\bar{\sigma}_{1,axial}$= 125 kPa), all stress curves have a bell shaped distribution. Although the shapes are more similar than above, the transmitted load is distributed more broadly again for the tests with geogrid spacings of 60 cm and 40 cm.

From the tests compared in this study, only the ones with a spacing of 20 cm and 40 cm have reached the third loading state of $\bar{\sigma}_{1,axial}$= 210 kPa. Both stress distributions have become slimmer due to evolving shear surfaces in the specimens underneath, as described in detail in Jacobs et al. (2012). As seen above, the test with a vertical layer spacing of 40 cm has led to the broadest load distribution, reducing the maximum local stress.

It might have been assumed that the load is transferred most uniformly when a geogrid layer was placed close to the position of loading. This has been the case for lower load levels, as shown in the upper two graphs where the 60 cm-spacing has led to a broader load distribution and therefore smaller maximum local stresses than the 20 cm-spacing. But in terms of the global ultimate bearing capacity, a higher value has been reached by the test with a layer spacing of 20 cm.

In total, being in line with the results from the above evaluation that accounts for the ultimate bearing capacity, the geogrid arrangement with a spacing of 40 cm has led to the best performance under the prevailing boundary conditions regarding the stress distribution. Generally, it can be said that for loading during service as well as for the ultimate limit state, the appropriate geogrid arrangement is of great importance. A test setup with a regular distribution of the reinforcement layers over the specimen height and the ratio of l_v/W = 0.5 seems to be the most appropriate geogrid arrangement for biaxial compression tests. All further tests, hence, have been carried out with two reinforcement layers placed at 1/4 H and 3/4 H.

Variation of Geogrid Tensile Stiffness

To investigate the influence of the tensile stiffness of the geogrids on the composite material, the stiffness has been varied in a common range between $J_{0\text{-}2\%}$ = 530 kN/m and 1650 kN/m. The resulting stress-strain and volumetric strain curves are presented in Fig. 6 and it can be seen that an increased tensile stiffness leads to a higher modulus

and a higher bearing capacity on one hand, and to delayed volumetric expansion on the other hand.

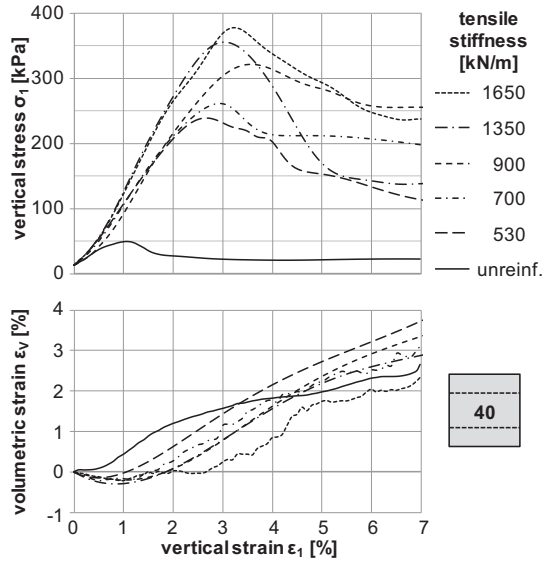

Fig. 6 Stress-strain and volumetric strain behavior of an unreinforced specimen and of specimens reinforced with two geogrid layers with a varying tensile stiffness.

In Fig. 7 the ultimate stresses $\sigma_{1,max}$ of all six presented tests have been drawn over the respective tensile stiffness $J_{0\text{-}2\%}$. The determined trend line has a decreasing slope, showing that the increase in strength corresponding to a specific increase in tensile stiffness is higher at a lower stiffness level. Therefore, the presented results indicate that the beneficial effect of an increased tensile stiffness decreases with a higher stiffness level.

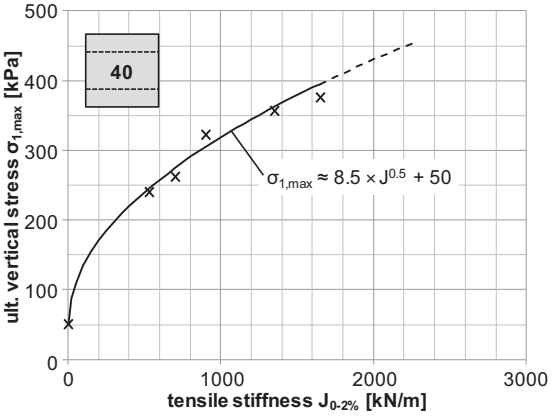

Fig. 7 Effect of the tensile stiffness of geogrids to the ultimate bearing capacity of the composite material.

The influence of a varying tensile stiffness of the geogrids on the kinematic behavior is shown in Fig. 8 where horizontal particle displacements and particle rotations are presented at the compression state of $\varepsilon_1 = 10$ %. For the specimen with the lowest geogrid tensile stiffness, the developed shear surfaces run almost straight through the geogrids, while for those tests with a higher tensile stiffness, in the vicinity of the geogrids the shear zones bend towards the direction of their tensile members. This can be explained by the simple fact that more energy is needed to strain the stiff geogrids. Therefore, the shear surfaces rather change their direction so that the soil slides along the geogrid than crossing it. This again corresponds to the determined higher relative displacements between geogrid and soil, which are not presented in this paper due to the limited space.

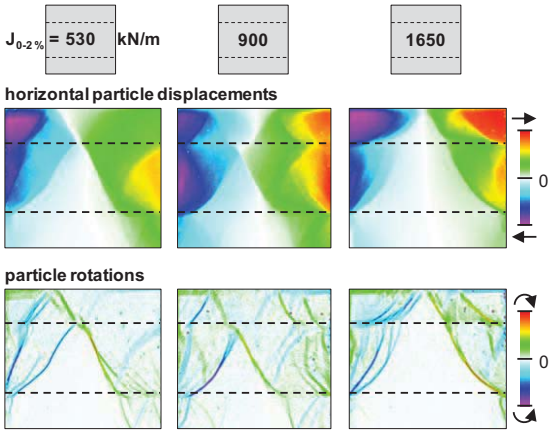

Fig. 8 Horizontal particle displacements and particle rotations of specimens reinforced with two geogrid layers with a different tensile stiffness at $\varepsilon_1 = 10$ %.

If those relative displacements would be reduced by e.g. a fixation of the geogrids at the σ_3-planes of the specimen (what is inhibited by the experimental boundary conditions), the sliding surfaces had to cross the stiff geogrids and by those means, more energy would have to be applied. For many in situ conditions the geogrids are at least partly fixed, e.g. by the connection to the facing of a retaining wall or by sufficient anchorage length in bearing layers, and therefore, the effect of an increased tensile stiffness is expected to be even more beneficial than shown in Fig. 7.

SUMMARY AND CONCLUSION

The presented results of large scale biaxial compression tests confirmed the expected increase in compound stiffness and bearing capacity of soil that is reinforced with geogrids. The large scale dimensions and the up-to-date and redundant measurement tools allowed a detailed investigation of the reinforcing effect.

An appropriate geogrid arrangement in the specimen was determined for the prevailing geometry and boundary conditions. Regarding the ultimate bearing capacity, the kinematic behavior, as well as the stress distribution on the specimen top surface, the best performance was achieved by a specimen with regularly distributed geogrids at 1/4 H and 3/4 H and the ratio of layer spacing to specimen width $l_v/W = 0.5$.

It could be shown that the vertical layer spacing is of great importance for the ultimate bearing capacity as well as for the stress distribution at all loading states. The challenging task in practice for designing bearing layers might be to determine an approximately regular geogrid arrangement for a given layer width, estimating the total effective bearing layer thickness. A suggestion can be drawn from the presented stress distributions; for a maximum ultimate bearing capacity the geogrids should rather be positioned towards the center of the layer. But if the performance of the bearing layer in the range of serviceability is the critical designing factor, the geogrids should rather be positioned towards the top of the layer, as it spreads the load and reduces the maximum local stresses at the layer surface.

As expected, an increase in the tensile geogrid stiffness led to an increased compound stiffness and higher bearing capacities of the reinforced soil. A convex relationship between the tensile stiffness and the ultimate vertical stress was determined, indicating that the beneficial effect of an increased tensile stiffness decreases at higher stiffness levels. However, for many in situ conditions, geogrids are expected to be at least partly fixed. In these cases, the beneficial effect shown in this study is expected to be exceeded with an increasing tensile stiffness of the geogrids.

ACKNOWLEDGEMENTS

The authors would like to thank Naue GmbH & Co. KG and Colbond bv for providing the geogrids and for their financial support. Special thanks go to the Geosynthetic Institute (GSI), PA, USA that also supported part of this work under its GSI Fellowship Program.

REFERENCES

ASTM Standard D2487 (2011). Standard Practice for Classification of Soils for Engineering Purposes (Unified Soil Classification System). ASTM International, West Conshohocken, PA, 2011, DOI: 10.1520/D2487-1, www.astm.org.

Bussert, F. (2006). Verformungsverhalten geokunststoffbewehrter Erdstützkörper – Einflussgrößen zur Ermittlung der Gebrauchstauglichkeit. Wissenschaftliche Schriftenreihe Geotechnik und Markscheidewesen. TU Clausthal, Heft 13, language: German.

Jacobs, F., Ruiken, A., and Ziegler, M. (2012). Investigation of geogrid reinforced soil with large scale "element" testing. GeoAmericas2012 – Proc. 2nd Pan American Congress Geosynthetics, Lima, Peru, 1-4 May 2012.

Ketchart, K. and Wu, J.T.H. (2001). Performance test for geosynthetic-reinforced soil including effects of preloading. U.S. Department of Transportation – Federal Highway Administration. Report No. FHWA-RD-01-018.

Peng, F.-L., Kotake, N., Tatsuoka, F., Hirakawa, D. and Tanaka, T. (2000). Plane strain compression behaviour of geogrid-reinforced sand and its numerical analysis. Soils and Foundations 40(3): 55-74.

Ruiken, A., Ziegler, M., Ehrenberg, H. and Höhny, S. (2010). Determination of the soil confining effect of geogrids. Proc. 14th Danube-European Conference on Geotechnical Engineering, Bratislava, Slovak Republic, 2-4 June 2010.

Ruiken, A., Jacobs, F., and Ziegler, M. (2012). Large scale biaxial compression testing of geogrid reinforced soil. EuroGeo5 – Proc. 5th European Geosynthetics Congress, Valencia, Spain, 16-19 September 2012.

Tatsuoka, F. and Haibara, O. (1985). Shear resistance between sand and smooth or lubricated surfaces. Soils and Foundations 25(1): 89-98.

Vidal, H. (1969). The Principle of Reinforced Earth. American Society of Civil Engineers: Geotechnical Special Publication (118, 2): pp. 1331-1346.